Soft Matter

Accepted Manuscript

ROYAL SOCIETY OF CHEMISTRY

www.rsc.org/softmatter

The effect of plastic rearrangements on the flow of two-dimensional wet foam

Zefeng Jing, Shuzhong Wang, Mingming Lv, Zhiguo Wang and Xiangrong Luo
Key Laboratory of Thermo-Fluid Science and Engineering of MOE, School of Energy and Power Engineering, Xi'an Jiaotong University, Xi'an, Shanxi, China

Abstract

The effect of the elementary plastic events on the flow behavior of the two-dimensional wet foam is investigated by the quasistatic simulation on the bubble scale. The position where the plastic event occurs is traced by recording the coordinate at which two bubbles separate in the simulation. Localized shear band is found, and the width of this band increases with the increase of foam quality. From the displacement fields of these bubbles, it shows that the T1 plastic events can give rise to an increase in local bubbles displacements due to the separation between these bubbles. The average relative pressure as well as normal stress difference of bubbles increases with the flow of foam in the initial elastic domain and then decreases as the elastic domain turns into the plastic domain. In the plastic domain, the plastic events rearrange the local structure of foam, which leads to decreasing both the average pressure and the normal stress difference. Additionally, the wall slip of foam is discussed in the simulation as well. The width of localized shear band is narrower under the slip boundary condition. Meanwhile, the plastic events occurring between the first and second layers of bubbles change the pulling force of the films near the wall and cause an instantaneous increase in the slip velocity.

1 Introduction

Liquid foam is a discrete system with discrete phase dispersed in continuous liquid phase. Its structure is maintained by both the surface tension of bubbles and the capillary pressure generated by geometry of the bubbles.[1, 2] As the foam flows, it can exhibit an intricate mixture of nonlinear viscous, elastic and plastic

behavior.[3, 4] This complex behavior is widely used in many industrial applications,[5] such as enhance oil recovery, ore flotation and cosmetic industry. As a result, it is of paramount importance to get a full understanding of the flow behavior of the wet foam.

In macroscopic view, the steady-state rheology of foam exhibits shear thinning and is generally described by the Herschel-Bulkley relation:[4, 6-8]

$$\dot{\gamma} = 0 \qquad \text{for} \quad \tau < \tau_y \tag{1}$$

$$\tau = \tau_y + K\dot{\gamma}^n \qquad \text{for} \quad \tau \geq \tau_y \tag{2}$$

where $\dot{\gamma}$ is the shear rate, τ_y the yield stress, n the power law exponent and K the consistency index. From this relation, it is easily known that the velocity profile of the foam presents a plug region in the middle of the circular tube in the case of Poiseuille flow.[9] In the other region, the foam displays shear flow with discrete topological rearrangements.

The topological rearrangement, called plastic event (T1), is a continuous evolutionary process. It is fundamental to the flow of foam. As shown in Fig. 1, with the shear flow of the wet foam, two threefold Plateau borders merge to form a fourfold Plateau border.[10] The fourfold Plateau border will persist until two of the Plateau border interfaces meet. Then a new air-liquid-air interface is formed between two threefold Plateau borders. Nevertheless, for the dry foam, four films meet at a point and then are resolved rapidly by the T1 event.[10] The T1 event for two-dimensional wet foam is different from the one for the dry foam in that the fourfold Plateau border can sustain in different forms (see Figs. 1(b), 1(c) and 1(d)) during the flow. At the microscopic level, the film of one bubble deforms owing to the interaction with the other. Since the foam is a nonuniform system, the elastic-plastic deformation of each film in the whole foam is different under shear condition. The link between the shear-induced deformation on the bubble scale and the resulting nonlinear dynamics response of the whole wet foam is not entirely resolved. A comprehensive

understanding of the bubble dynamics entails a detailed description of the deformation of foam structure.[11] Katgert *et al.*[11] investigated the flow in linearly sheared two-dimensional foam sandwiched between a liquid bath and glass plate on the bubble scale. Through analyzing the inhomogeneous velocity profiles, they found that the shear band appeared in both the ordered and disordered foams. However, they could not record the plastic events and thus would not obtain the role of T1 events in the velocity profiles. Therefore, in the present work, one objective is to gain the effect of the T1 events on the flow dynamics of two-dimensional wet foam from the bubble scale through focusing on the plastic events (T1s). On the other hand, because of both the inhomogeneity of foam structure and the discrete T1 events, the validity of the Herschel–Bulkley relation for flowing foam has been called into question on the bubble scale.

As the foam flows, the characteristic parameters of a foam sample, such as the elasticity[12, 13] and pressure level, change constantly. Although Gardiner *et al.*[13] adopted Soft-disk model of Durian[14] to research the evolution of normal stress difference of wet disordered foams in pure shear, the results, from geometry view, were not very convincing for both the non-deformation of the bubble structure and overlap among the bubbles in the Soft-disk model. As a matter of fact, the foam structure reveals its characteristic parameters. Meanwhile, the irreversible plastic events (T1s) rearrange the local structure of a foam sample. The rearrangements then affect these characteristic parameters. Therefore, one objective of the present study is to explore the link between the plastic events and the evolutions of both the normal stress difference and the pressure of the flowing wet foam.

On the other hand, the continuous flow of foam is usually affected by wall slip which is rather general in this system.[15, 16] At the microscopic level, the deformable bubble films are generally larger than the dimensions of the wall corrugations, which allows them to surpass these corrugations. In this case, the friction between the films and solid wall was generally studied.[16] With this in mind, several models, such

as Bretherton's model[17] and Denkov's model,[16] were developed. Nevertheless, in these studies, the effect of the plastic event was not taken into consideration. Actually, the deformation of films will change when the T1s occur near the wall. It is still unclear exactly how this change affects the slip of the foam. Thereby, the last objective in this paper is to explore the relationship between the plastic events and the wall slip of the foam.

To attain these research objectives, firstly, the distribution characteristics of T1s are studied in the flow simulation. Secondly, combining with the T1 events, we analyze the evolutions of bubbles displacements, average pressure and elasticity on the bubble scale. Thirdly, the slip boundary condition based on the bubble films is introduced into the flow simulation, and then the effect of T1s on the slip velocity is observed. To summarize, the paper is organized as follows: Sec. 2 describes the foam model. Sec. 3 and Sec. 4 present both the results and analysis based on the no-slip boundary condition and the slip boundary condition, respectively. Sec. 5 summarizes the conclusions.

2 Numerical model

In general, simulations of foam rheology fall into two categories: quasistatic model, such as large Q-Potts model,[18] 2D-Froth model[19] and Surface Evolver method,[20] and non-quasistatic model, such as Lattice gas method[21], Vertex model[22] and Soft-disk model[8, 14]. Quasistatic model of the foam is composed of equilibrium structures of the foam. The main assumption of the quasistatic model is that the relaxation rate of the foam is much higher than both the shear rate and the diffusion rate of the foam. In other words, the deformation of the foam is so slow that the viscous effect can be negligible. The large Q-Potts model uses rectangular lattice sites with the same digital to approximate a foam structure[18]. Yet, it cannot accurately represent a foam structure due to these rectangular lattice sites. For the 2D-Froth model,[19] the main disadvantage is that it is only used for dry foam. Lattice Gas model, adopted by Sun and Hutzler[21] to

simulate liquid foam, is confined to a small number of bubbles. Furthermore, energy dissipation of the foam does not include the one caused by the T1s in the Lattice Gas model. The Vertex model was developed to study foam rheology by Okuzono *et al*.[22]. However, the Vertex model does not reflect the real bubble structure since the edges of the foam are straight line and cannot be applied to the related simulation of the wet foam. In the Soft-disk model of Durian[14], the bubble structure is represented approximatively as a circular disc. It does not represent the foam by a realistic structure. The circular disc is allowed to overlap[8], and the foam structure will become increasingly less realistic with the decrease of liquid fraction. The Surface Evolver provides a necessary framework within which to perform quasistatic simulation of both dry and wet foams. Moreover, a further important feature in the Surface Evolver is the ability to perform T1s.

The Surface Evolver[20] is specialized to minimize the total energy of surfaces subject to user defined constraints by changing the coordinates of the vertices. The equilibrium structure of the 2D foam is obtained by minimizing the length of the bubbles films while maintaining the target area of each bubble. Therefore, the energy constraint of a 2D wet foam can be written as:

$$E = \gamma \sum_i l_i + \sum_k p_k (A_k - A_k^t) \tag{3}$$

where γ is the line tension of the films, l_i the length of the foam's films, p_k the pressure of the bubble k, A_k current area of bubble k and A_k^t the constrained target area.

In the wet foam, there are two types of interfaces: air-liquid-air interfaces between neighboring bubbles and air-liquid interfaces between bubbles and Plateau borders (see Fig. 2). As shown in Fig. 2, the contact angle α between the two different types of interfaces can be given by

$$\alpha = \cos^{-1}(\frac{\gamma_1}{2\gamma_2}) \tag{4}$$

The non-zero contact angles can arise in liquid foam.[23] Therefore, in order to keep the contact angle

small and make contacts more well-behaved in our simulation, the tension of air-liquid-air interfaces γ_1 is set to 0.99 and the tension of air-liquid interfaces $\gamma_2 = 0.497$.

The bubbles will overlap (see Fig. 3(a)) when the foam flows. Nevertheless, the detection of overlap is not something that Surface Evolver can do automatically. Therefore, a script is written to detect and handle the overlap. As displayed in Fig. 3, the script starts at a triple vertex and follows edges around the void to see whether two edges intersect. If the intersection is found, the vertice is created at the intersection. The overlapping between the bubbles is then collapsed to a single edge. Due to the set area constraint of each bubble in the foam sample, both the area of each bubble and the liquid fraction of the whole foam will remain unchanged when the equilibrium configuration of the foam is obtained at each iteration. Therefore, the script does not bring some systematic errors.

For disordered polydisperse foam, the bubbles sizes are allocated randomly according to a Lognormal Distribution with the probability density function:[24]

$$f(x;\mu,\sigma) = \frac{1}{x\sigma\sqrt{2\pi}} e^{-(\ln x-\mu)^2/2\sigma^2} \tag{5}$$

where μ is the expectation which denotes the average bubble size and σ^2 is the variance which denotes the disorder of a foam sample. It will be monodisperse foam at $\sigma^2 = 0$. According to the size of foam channel and the number of bubbles in simulation, the expectation μ is set to 0.0254. For the foam with medium disorder, the variance σ^2 can be set to 0.2. To create a wet foam system, an equilibrium dry foam (the limit $\Phi_g \to 1$) structure is created first, and a periodic boundary condition is retained at the right and left of the channel. Meanwhile, the vertices of films that join either wall are fixed so that a no-slip boundary condition is imposed.

In the two-dimensional wet foam, the liquid is mainly contained in Plateau borders. Therefore, as shown in Fig. 4, the area of Plateau borders can be referred to as the liquid fraction of the foam, and the fraction of

the gas phase in foam is also called foam quality Φ_g. The target area of each bubble in the equilibrium dry foam is multiplied by Φ_g according to the given foam quality. Then each threefold vertex is replaced by a threefold Plateau border (see Fig. 2) in the bulk foam. Subsequently, the equilibrium configuration of the wet foam with the foam quality Φ_g is obtained by both the gradient descent method and the conjugate gradient method.

To make the simulation convenient, the default system of units in the Surface Evolver is adopted. As displayed in Fig. 4, one red line (i.e., the line a) on the y axis is fixed, which ensures it not moving, and the other red line of bubbles films (i.e., the line b) connecting the two walls is chosen at random. The two red lines join the lines along the channel walls, which defines a region with a certain area A_0. In the simulation, the area of this region is constrained. The method to drive the bubbles to flow is that the target area of this region is enlarged by a same amount $\delta A_0 = 0.0007$ at each iteration, which can be considered as the pipe flow with a constant flow rate; then the equilibrium structure of the foam is obtained by the conjugate gradient method. In addition, the red line of bubbles films will be reselected once the T1 event occurs in the red line of bubbles films. In future, we can build two-dimensional foam sandwiched between a liquid bath and glass plate. By means of the high-speed photography technology and image analysis, the effect of the plastic events on the detailed flow of the two-dimensional wet foam is investigated experimentally.

3 Description of the flow behavior

3.1 Shear localization

Shear band is a common phenomenon in non-Newtonian fluid. There are two or more co-existing regions of fluid flowing in bands at different shear rates. The shear band of the flowing foam has been observed in experiments[11, 25, 26] and numerical simulations.[27, 28] Nevertheless, the simulation of the shear band on the foam is generally restricted to the two-dimensional dry foam (the limit $\Phi_g \rightarrow 1$). As the foam

flows, it experiences a series of T1 topological events that modify its structure. Accordingly, the shear band can be characterized by localization of T1s. The coordinate where two bubbles separate at the initial phase of the T1 event is recorded in simulation. The *y*-coordinates of the T1s versus the iteration number for different foam qualities are given in Fig. 5. It is clear that the T1s mainly occur near the channel walls.

The number of T1s found in the upper and lower halves of the channel is counted, respectively. In order to describe the shear localization, we adopt the same procedure described by Cox and Wyn.[29] The distance w_d from the lower wall within which 90% of the T1s in the lower half of the channel occur and the distance w_u from the upper wall within which 90% of the T1s in the upper half of the channel occur are calculated, respectively. In Fig. 5, combining the distances w_d and w_u and subtracting the average diameter of the bubbles, the width of the localized shear region w_l can be defined as:

$$w_l = w_d + w_u - 2\sqrt{\frac{4\overline{A}}{\pi}} \tag{6}$$

where $\overline{A}$ is the average bubble area. The width of the localized shear region w_l of the foam for different foam qualities is illustrated in Table 1. From Table. 1, it is obviously shown that the width w_l increases with foam quality Φ_g. However, the accurate relationship between the width and the foam quality should be investigated in future under many different values of both disorder and foam quality conditions.

Table 1 The width of the localized shear region w_l, normalized by the square-root of the average area $\overline{A}$, with respect to the foam quality.

Φ_g	88%	90%	92%	94%
$w_l / \overline{A}^{1/2}$	3.8140	4.3643	4.8081	5.7539

3.2 Displacement field

The center coordinate of each bubble is recorded when an equilibrium configuration of the foam is obtained at each iteration. Displacements of these bubbles centers in different iteration intervals are

presented by arrows in Fig. 6.

In order to show the effect of T1 events on the displacement of these bubbles, the variation rate of average bubbles displacements along *y* direction is introduced. The displacement of the bubble can show the size of its velocity *u* in the iteration interval (i.e., time Δt). In this way, it can be obtained that the slope of the curve of average bubbles displacements versus *y*-coordinates reflects the size of the variation rate which can be deemed to the shear rate according to the formula:

$$\dot{\gamma} = \frac{du}{dy} \tag{7}$$

As displayed in Fig. 6(a), the profile of the average displacement is a combination of curves in sheared regions, i.e., those regions with non-zero local strain rate, and a plug in non-sheared region, i.e., the middle part of the foam channel where the profile is similar to a plug flow. This plug flow of foam agrees with the Herschel-Bulkley fluid. However, as illustrated in Fig. 6(b), the curve of average displacement changes rapidly, and the shear rate reaches a maximum value in the upper part of the foam channel accordingly. It presents an asymmetric flow, and the curve is completely different from the velocity profile of the Herschel-Bulkley fluid. The asymmetric flow of foam is also found in early work.[30] From Fig. 7 and the displacement field in Fig. 6(b), it is obvious that the more T1s occur in the upper part of the channel during this interval and lead to an increase in local bubbles displacements in this region. Unlike homogeneous Newtonian and non-Newtonian fluids, the disordered foam, whose structure is asymmetric, is a discrete system, which leads to the asymmetric flow. From the microscopic level, due to the disordered structure of foam, the force on each bubble in this system changes as the foam flows. This changing force leads to significant change in the displacement field. As the T1 event appears, the film between neighboring bubbles disappears (see Figs. 1(a) and 1(b)), and then one bubble slips the leash from the other, which causes a decrease in the flow resistance. The less the flow resistance acts on the bubble, the more easily it

moves. Therefore, the bubble near the T1 event will move faster along the flowing direction when the T1 event occurs.

3.3 Bubble pressure and normal stress difference

The pressure inside the bubble changes as the foam sample undergoes elastic-plastic deformation in the simulation. The relative pressure of a bubble to the continuous liquid phase can be given by Surface Evolver as the Lagrange multiplier of the area constraint on each bubble. As shown in Fig. 8(b), compared with the initial foam (see Fig. 8(a)), the pressure level of bubbles on the right of the red line increases. However, in Fig. 8(c), the bubbles with higher pressure are less than the ones in Fig. 8(b), which indicates that the average pressure of these bubbles decreases. In order to describe the pressure change of these bubbles, the average relative pressure $\bar{p}$ of these bubbles is defined as:

$$\bar{p} = \frac{1}{n}\sum_{i=1}^{n} p_i \tag{8}$$

where n is the total number of bubbles and p_i denotes the relative pressure of bubble i. The evolution of the average relative pressure $\bar{p}$ versus the iteration number is illustrated in Fig. 9(a). It demonstrates that the average pressure initially increases with the iteration number and then shows a downward trend.

The foam also shows different stress states depending on its deformation. At strains below the yield strain, the foam behaves as an elastic solid, and above the yield strain, it occurs irreversible plastic events. Dennin[31] used two-dimensional bubble rafts in a Couette geometry to study the response of stress to the T1s. In his experiment, the bubble rafts were subjected to slow steady shear. Then it showed that the correlation between the T1s and stress was not obvious during the initial elastic response while the T1s caused a drop in the stress during the subsequent plastic flow. However, the more geometric considerations about the connection between the T1s and stress drops are scarce in his analysis. As a matter of fact, the stress of these bubbles can change as the foam appears elastic-plastic deformation. The stress tensor in the

two-dimensional foam can be obtained by integrating the tension forces along each edge.[32]

$$\boldsymbol{\tau} = \begin{pmatrix} \tau_{xx} & \tau_{xy} \\ \tau_{yx} & \tau_{yy} \end{pmatrix} = \gamma \sum_{edges} \int_{\theta_1}^{\theta_2} \begin{pmatrix} \cos^2\theta & \sin\theta\cos\theta \\ \cos\theta\sin\theta & \sin^2\theta \end{pmatrix} R d\theta \tag{9}$$

where R denotes the radius of curvature of each edge, θ_1 is angle between the tangent of one endpoint of the edge and the positive direction of the x axis and θ_2 is angle between the tangent of the other endpoint of the edge and the positive direction of the x axis. Subtracting the initial value $\tau_{xx}^0 - \tau_{yy}^0$, the evolution of the normal stress difference is obtained:

$$\Delta\left(\tau_{xx} - \tau_{yy}\right) = \left(\tau_{xx} - \tau_{yy}\right) - \left(\tau_{xx}^0 - \tau_{yy}^0\right) \tag{10}$$

The normal stress difference $\Delta\left(\tau_{xx} - \tau_{yy}\right)$ can describe the evolution of elasticity in a foam system. Fig. 9(b) displays the evolution of the normal stress difference of the foam with respect to the iteration number. It is shown that the normal stress difference initially increases with the iteration number. The domain within which the normal stress difference increases can be referred to as the elastic domain. In this domain, the elastic deformation of the foam is mainly observed. Nevertheless, when the elastic deformation exceeds the elastic limit, the flow of foam will enter into the plastic domain within which more plastic events occur near the wall (see Fig. 5) and give rise to decreasing normal stress difference (see Fig. 9(b)). These results are in good agreement with the experimental results obtained by Dennin.[31]

As the foam flows, both the elastic deformation and the plastic rearrangement have influence on the normal stress difference as well as pressure of these bubbles. From Figs. 9(a) and 9(b), it can be obviously seen that the evolution of the average relative pressure is in sync with the normal stress difference in the initial elastic domain. In this domain, the elastic deformation of the whole foam caused by squeezing or stretching between these bubbles plays a major role in the increase of these two parameters. Although there are T1s in this domain, the contribution of the increasing elastic deformation is primary. This result is consistent with the experiment of Dennin.[31] Subsequently, the average pressure, as well as the normal stress

difference, starts to decrease at the transition from elastic to plastic domain. In order to illustrate the effect of T1 events on both the relative pressure level and the normal stress difference, the distribution of the number of T1s versus the iteration number is displayed in Fig. 9(c). It is clear that there is a significant drop in both these parameters when the T1s occur in the plastic domain. The T1 events change the local structure of the foam (see Figs. 1(a), 1(b) and 1(c)), which makes the mean curvature K of these bubbles films decrease. Therefore, according to the Laplace-Young law[33] $\Delta p = 2\gamma K$, the relative pressure level of these bubbles decreases, and because of decreasing elastic deformation of these bubbles films caused by stretching between these films, the normal stress difference also decreases. Furthermore, the Plateau border with four or more sides is a continuous evolutionary process when the T1s occur. The curvature K and elastic deformation of the bubble film gradually decrease in the initial stage of a plastic event (see Figs. 1(b) and 1(c)). As a consequence, these two parameters will continue to fall after two bubbles separate, which is obviously shown during 420-510 iterations in Fig. 9(a). Nevertheless, these two parameters present a different trend during 510-680 iterations in Fig. 9. This phenomenon can be attributed to elastic deformation of the whole foam sample in this domain. In the initial phase of this domain, the increasing elastic deformation of the whole foam makes the normal stress difference increase but is not enough to increase the average pressure of these bubbles when compared with the evolutionary plastic rearrangement.

4 Wall slip flow

Some experiments have confirmed the existence of the wall slip phenomenon in the foam system.[16, 34, 35] In these studies, the foam slides along the liquid film on the wall. The slip behavior can be investigated on the bubble scale through the numerical model method. As illustrated in Fig. 10, the bubble film near the wall displays distorted, and accordingly the contact angle α_w between the film and the wall will change when the foam flows. It can be considered that the slip motion is governed by dynamic friction. As the

foam flows, the distortional bubble film will provide a pulling force that drives the film on the wall to slide in the flow direction. Therefore, a balance of forces in the flow direction can be obtained:

$$\mu_f u_s = \sum_i \gamma_i \cos \alpha_{wi} \tag{11}$$

where μ_f is the coefficient representing the friction between the film and the wall, u_s the slip velocity that bubbles slide along the wall, γ the tension of the film and i the number of films that join either wall.

The slip boundary condition is introduced into the flow simulation. In the simulation, the friction coefficient can be set to different values representing different wall roughness. The pulling force of films that join either wall in the flow direction is measured when an equilibrium configuration of the foam is obtained at each iteration. Then the slip velocity can be calculated by Eq. (11). Thus, for each iteration ($\Delta t = 1$), the bubbles are moved a small displacement u_s. Meanwhile, the flow is implemented by the method described in Sec. II. Figs. 11(a) and 11(b) show the y-coordinates of the T1 events versus the iteration number under the friction coefficient $\mu_f = 5000$ and $\mu_f = 10000$, respectively. It is illustrated that the T1 events also mainly occur near the walls under the slip boundary condition. The width of localized shear region w_l for different friction coefficients is presented in Table 2. For the no-slip boundary condition ($\mu_f \to \infty$), the y-coordinates of the T1 topological events are shown in Fig. 5(b). From Table 2, it is clear that the width w_l increases with the friction coefficient. For the full-slip boundary condition ($\mu_f = 0$), since there is no relative motion among these bubbles, there is no shear localization.

Table 2 The width of localized shear region w_l for different friction coefficients.

μ_f	5000	10000	∞(no-slip)
w_l	0.577	0.676	0.687

In order to investigate the effect of T1 events occurring between the first and second layers of bubbles near the wall on the slip velocity, the distribution of the number of T1 events near the walls, as well as the variation of the rate of slip velocity to the average bulk velocity versus the iteration number is illustrated in

Fig. 12. It shows that the T1s occurring between the first and second layers of bubbles can cause an instantaneous increase in the slip velocity. According to Fig. 6, it can be obtained that the T1s can lead to an increase in local velocity of bubbles. The average velocity of the second layer of bubbles near the wall reaches a high level when T1s mainly occur between the first and second layers of bubbles. The second layer of bubbles can impel the bubbles on the wall to slip and, thus the slip velocity increases. Furthermore, as seen from Fig. 12, the slip velocity on the upper wall of the channel is different from the one on the lower wall due to the nonhomogeneity of foam structure.

5 Conclusions

The Surface Evolver method has been applied to the flow of the two-dimensional wet foam. The script that detects and handles the overlapping between the bubbles is added to the flow simulation, during which the geometrical deformation of the bubble caused by squeezing or stretching can be directly observed. These obtained results can reveal the response of flowing wet foam to the plastic events in meso-level. These contribute to have a deeper understanding of the flow behavior of this discrete system, such as foam and emulsion. It can be considered as a complement to a wider soft matter community.

It has been shown that the T1 plastic events mainly occur near the wall. The width of the localized shear region tends to increase with the foam quality. From the displacement fields of bubbles, it is illustrated that the T1 plastic events can lead to an increase in bubbles displacements in the localized region. On the bubble scale, due to the disordered structure of the foam, the displacement distribution of the foam versus y-coordinates during the certain iteration intervals does not meet the distribution of Herschel–Bulkley fluid. In the initial elastic domain, both the average pressure and the normal stress difference of these bubbles gradually increase as a result of the elastic deformation of the bubble, while in the plastic domain, the T1s cause a decrease in both these parameters. Subsequently, the trend of decrease will keep for a few iterations

on account of the evolutionary Plateau borders with four or more sides.

The pulling force generated by the bubbles films that join either wall is taken into account in the flow simulation. Combining the dynamic friction caused by slip motion of the bubbles at the walls, the balance of forces can be obtained. The band of T1s near the wall is narrower under the slip boundary condition. Meanwhile, it also shows that the plastic events near the wall can give rise to an instantaneous increase in the slip velocity. The work is now ongoing to research systemically the response of both the monodisperse and polydisperse foams to the wall slip by experiments and numerical simulation methods.

Acknowledgements

We would like to thank K. Brakke for assistance with the Surface Evolver method and S. J. Cox for the useful prompting for the flow of the two-dimensional foam. We are also grateful to C.C. Feng, D.H. Xu, Y. Guo and X.J. Zhang for fruitful discussions.

References

1. V. Reidenbach, P. Harris, Y. Lee and D. Lord, *SPE Production engineering*, 1986, **1**, 31-41.

2. A. Huerre, V. Miralles and M.-C. Jullien, *Soft Matter*, 2014, **10**, 6888-6902.

3. D. Weaire and S. Hutzler, *The physics of foams*, Clarendon Press, 1999.

4. R. Höhler and S. Cohen-Addad, *Journal of Physics: Condensed Matter*, 2005, **17**, R1041.

5. W. R. Rossen, *Surfactant Science Series*, 1996, 413-464.

6. R. G. Larson, *The structure and rheology of complex fluids*, Oxford university press, New York, 1999.

7. D. Weaire, *Current Opinion in Colloid & Interface Science*, 2008, **13**, 171-176.

8. M. Sexton, M. Möbius and S. Hutzler, *Soft Matter*, 2011, **7**, 11252-11258.

9. N. M. Wereley, *Journal of Intelligent Material Systems and Structures*, 2008, **19**, 257-268.

10. H. Princen, S. Friberg, K. Larsson and J. Sjöblom, *Food emulsions*, 2004, 413-483.

11. G. Katgert, A. Latka, M. E. Möbius and M. van Hecke, *Physical Review E*, 2009, **79**, 066318.

12. A. Kabla and G. Debregeas, *Journal of Fluid Mechanics*, 2007, **587**, 23-44.

13. B. Gardiner, B. Dlugogorski and G. Jameson, *Journal of non-newtonian fluid mechanics*, 2000, **92**, 151-166.

14. D. J. Durian, *Physical Review Letters*, 1995, **75**, 4780-4783.

15. A. M. Kraynik, *Annual Review of Fluid Mechanics*, 1988, **20**, 325-357.

16. N. D. Denkov, V. Subramanian, D. Gurovich and A. Lips, *Colloids and Surfaces A: Physicochemical and Engineering Aspects*, 2005, **263**, 129-145.

17. F.P. Bretherton, *Journal of Fluid Mechanics*, 1961, **10**, 166-188.

18. Y. Jiang, P. J. Swart, A. Saxena, M. Asipauskas and J. A. Glazier, *Physical Review E*, 1999, **59**, 5819-5832.

19. J. P. Kermode and D. Weaire, *Computer Physics Communications*, 1990, **60**, 75-109.

20. K. A. Brakke, *Experimental mathematics*, 1992, **1**, 141-165.

21. Q. Sun and S. Hutzler, *Rheologica acta*, 2004, **43**, 567-574.

22 T. Okuzono and K. Kawasaki, *Physical Review E*, 1995, **51**, 1246-1253.

23. I. Ivanov, A. Dimitrov, A. Nikolov, N. Denkov and P. Kralchevsky, *Journal of colloid and interface science*, 1992, **151**, 446-461.

24. G. Marion, S. Sahnoun, B. Mendiboure, C. Dicharry and J. Lachaise, in *Trends in Colloid and Interface Science VI*, eds. C. Helm, M. Lösche and H. Möhwald, Steinkopff, 1992, vol. 89, ch. 33, 145-148.

25. Y. Wang, K. Krishan and M. Dennin, *Physical Review E*, 2006, **73**, 031401.

26. J. Lauridsen, G. Chanan and M. Dennin, *Physical Review Letters*, 2004, **93**, 018303.

27. A. Kabla and G. Debrégeas, *Physical review letters*, 2003, **90**, 258303.

28. A. Kabla, J. Scheibert and G. Debregeas, *Journal of Fluid Mechanics*, 2007, **587**, 45-72.

29. S. Cox and A. Wyn, AIP Conf. Proc., 2008, **1027**, 836-838.

30. V. J. Langlois, *Journal of Rheology*, 2014, **58**, 799-818.

31. M.Dennin, *Physical Review E*, 2004, **70,** 041406.

32. Z. Jing, , S. Wang, , M. Lv, Z. Wang and X. Luo, *Journal of Fluids Engineering-Transactions of the ASME*, 2014. (in press).

33. D. Weaire and R. Phelan, *Journal of Physics: Condensed Matter*, 1996, **8**, 9519.

34. A. M. Loureno, S. Z. Miska, T. D. Reed, M. B. Pickell and N. E. Takach, *SPE Drilling & Completion*, 2004, **19**, 139-146.

35. N. D. Denkov, S. Tcholakova, K. Golemanov, K. Ananthpadmanabhan and A. Lips, *Soft Matter*, 2009, **5**, 3389-3408.

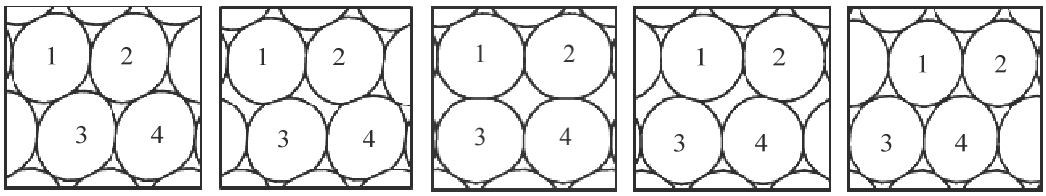

(a) (b) (c) (d) (e)

Fig. 1 The T1 event for a two-dimensional wet foam. This topological rearrangement results in neighbor swapping between two pairs of bubbles. Bubbles 2 and 3 were initially adjacent to each other. Subsequently, bubbles 1 and 4 become neighbors after the T1 event.

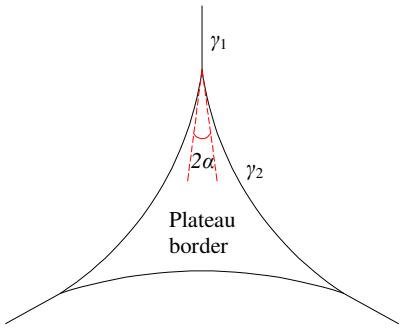

Fig. 2 A threefold Plateau border. The contact angle α is determined by the tension of air-liquid-air interfaces γ_1 and the tension of air-liquid interfaces γ_2.

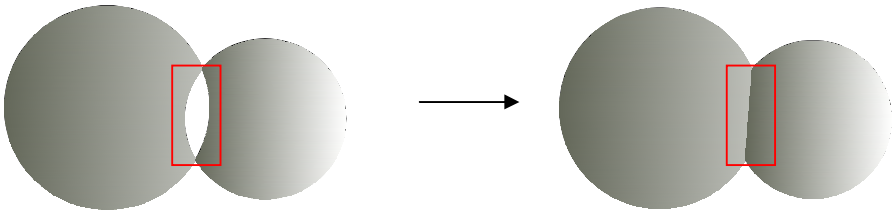

Fig. 3 The way to deal with the overlapping between the bubbles. The overlapping region is collapsed to a single edge. In the actual simulation, the overlapping region is very small and the length of edge that the overlapping region turns into is at 10^{-3} order of magnitude.

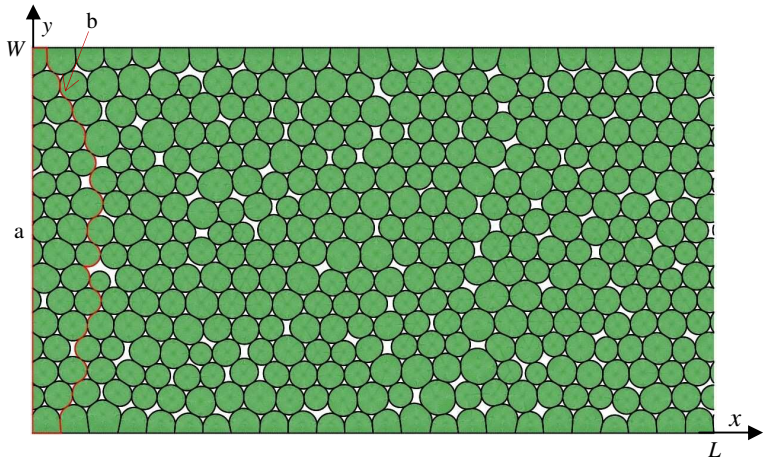

Fig. 4 Example of wet foam with $\Phi_g = 0.90$ between parallel walls. The Plateau borders with more than four sides are presented in this foam sample. W represents the width of the foam channel and L the length of the foam channel. The periodic boundary condition is maintained in the x direction. In the simulation, $W = 2.350$ and $L = 4.157$. The red line a is on the y axis and the red line b represents the continuous bubbles films connecting the two walls.

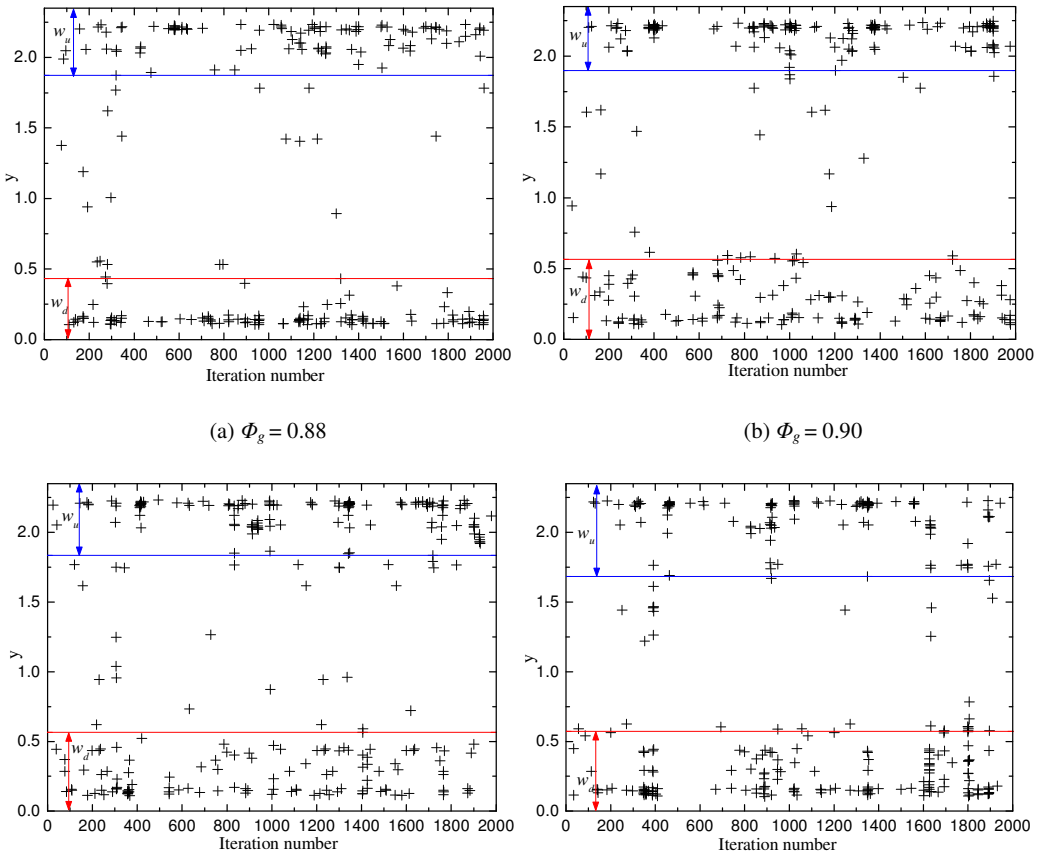

(a) $\Phi_g = 0.88$ (b) $\Phi_g = 0.90$

(c) $\Phi_g = 0.92$ (d) $\Phi_g = 0.94$

Fig. 5 The y-coordinate of each T1 topological event versus the iteration number for the foam with different foam qualities.

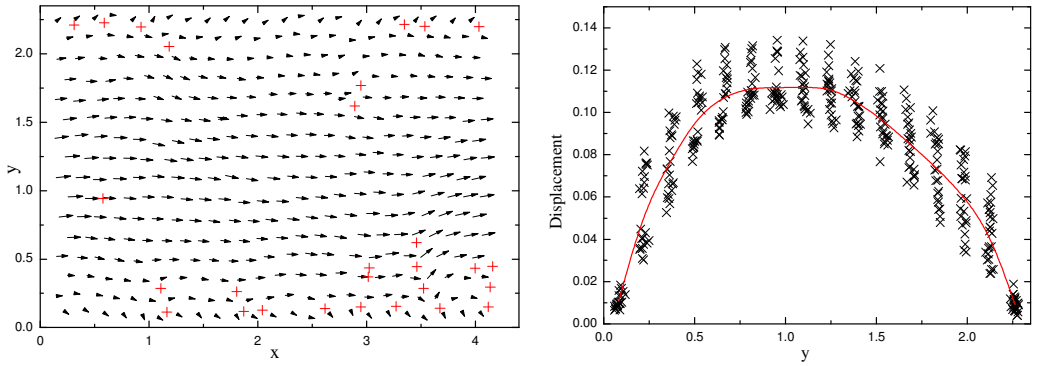

(a)

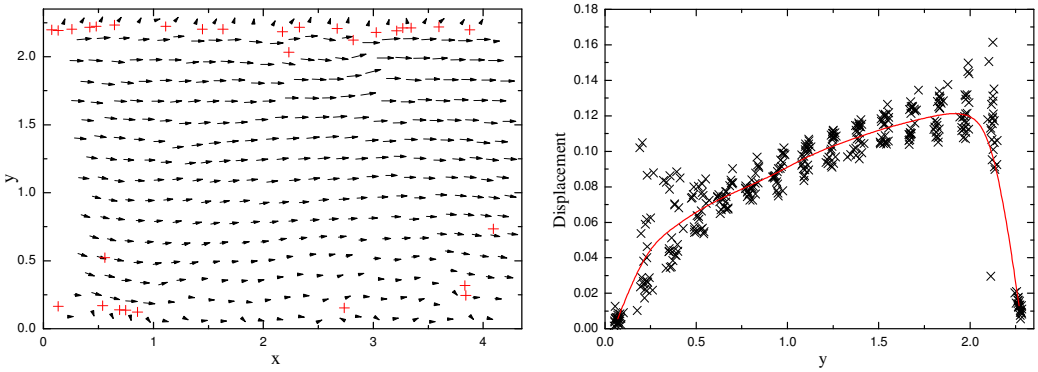

(b)

Fig. 6 Displacement fields and displacement size of each bubble corresponding to the left displacement fields during (a) 0-300 iterations and (b) 400-700 iterations for the foam with $\Phi_g = 0.92$. The red plus signs in the displacement fields show the coordinates of T1s in these iteration intervals. The detailed distribution of the number of T1s during 400-700 iterations is shown in Fig. 7. The *y*-positions of T1s versus iteration number are shown in Fig. 5(c). The red curves display average displacements of the bubbles at approximate y-coordinates versus y-positions in these iteration intervals.

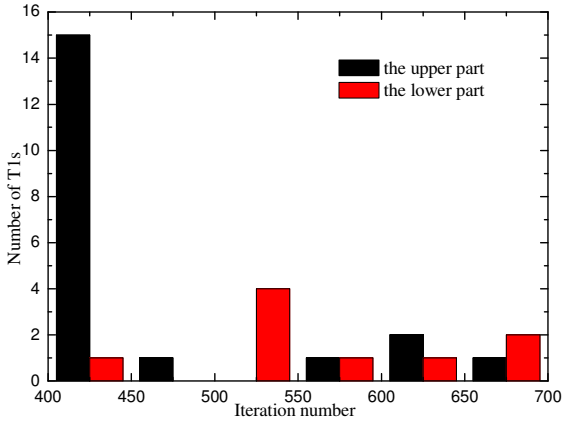

Fig. 7 Distribution of the number of T1s occurring at each interval of 50 iterations in the upper and lower parts of the foam channel during 400-700 iterations for the foam with $\Phi_g = 0.92$. It is easily seen that the total number of T1s in the upper part of the channel is greater than that in the lower part.

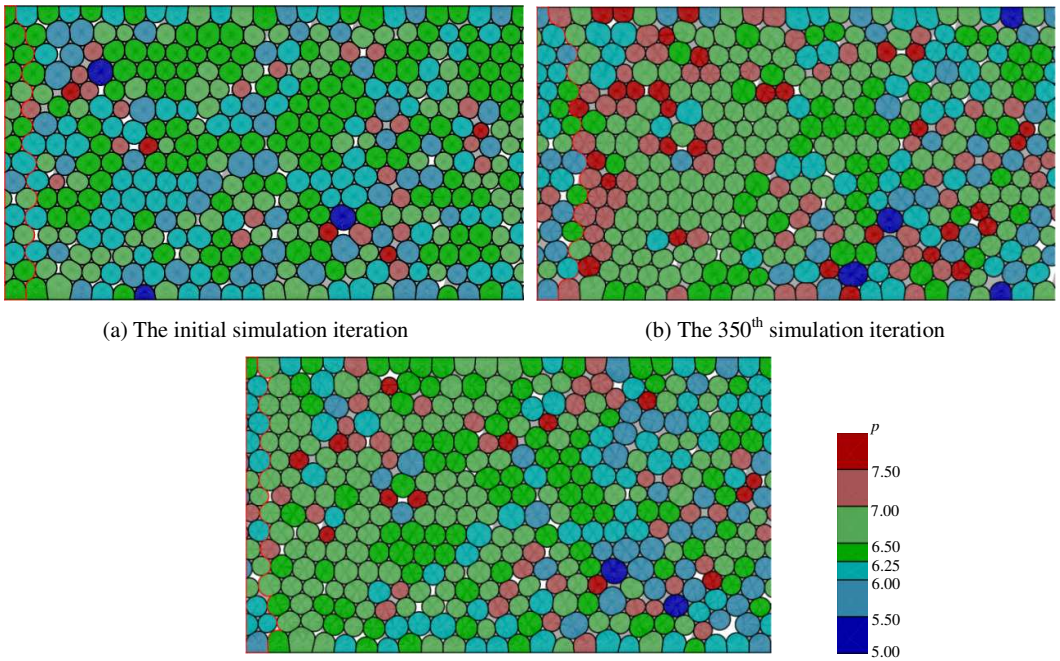

(a) The initial simulation iteration

(b) The 350th simulation iteration

(c) The 600th simulation iteration

Fig. 8 The bubbles are colored depending on their relative pressure which is related to the curvature of their films. The pressure increases with the order blue, light blue, cyan, green, light green, light red to red. Each figure represents pressure field of the foam with $\Phi_g = 0.92$ under different iteration number. These pressure fields also demonstrate the non-uniform pressure distribution in a foam system.

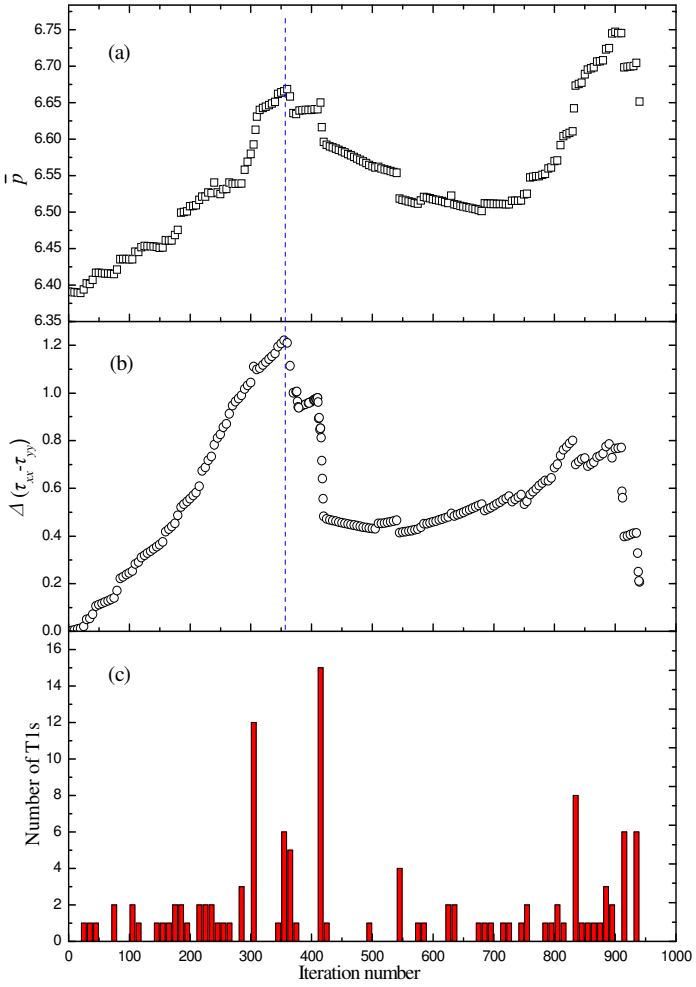

Fig. 9 Evolutions of (a) average relative pressure and (b) normal stress difference of the foam with foam quality Φ_g = 0.92 versus the iteration number. (c) Distribution of the number of T1s versus the iteration number. The distribution of T1s is shown in Fig. 5(c). The vertical dotted line is located at the transition from elastic to plastic domain.

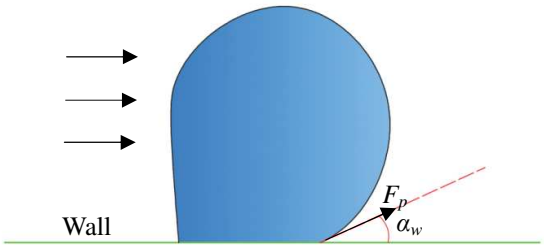

Fig. 10 A contact angle α_w between the bubble film and the wall. The parallel arrows point to the flowing direction. The force F_p denotes the pulling force provided by the bubble film.

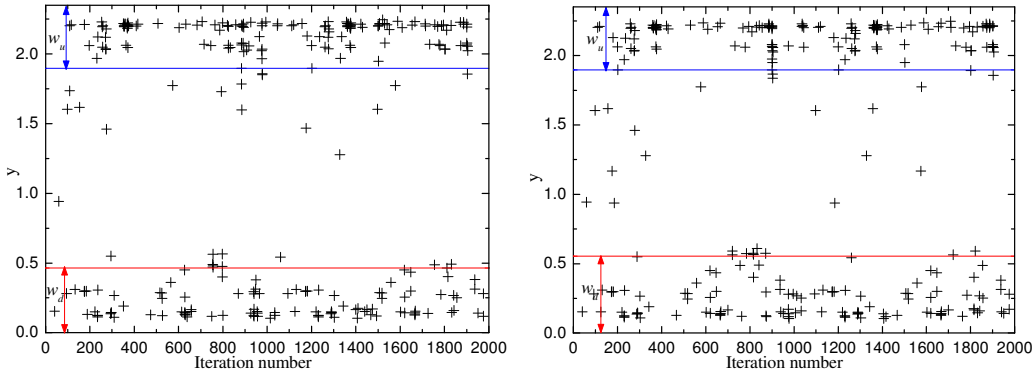

(a) (b)

Fig. 11 The *y*-coordinates of the T1 topological events versus the iteration number for foam with $\Phi_g = 0.9$ under the slip boundary condition. The friction coefficient (a) $\mu_f = 5000$ and (b) $\mu_f = 10000$.

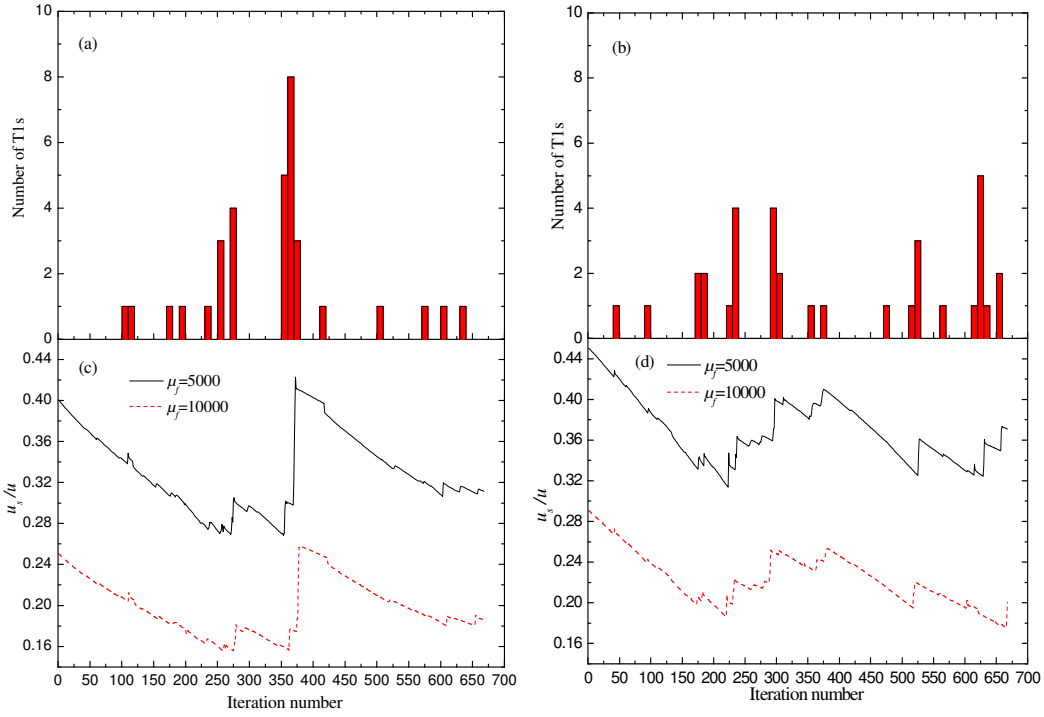

Fig. 12 Histograms showing the evolution of the number of T1s occurring near (a) the upper wall and (b) the lower wall versus the iteration number. The friction coefficient is $\mu_f = 5000$ and the foam quality $\Phi_g = 0.9$. The distribution of T1s is shown in Fig. 11(a). The curves show the evolution of the rate of slip velocity of bubbles on the (c) upper and (d) lower walls to the bulk velocity. It can be clearly seen that the smaller the wall roughness, the higher slip velocity.

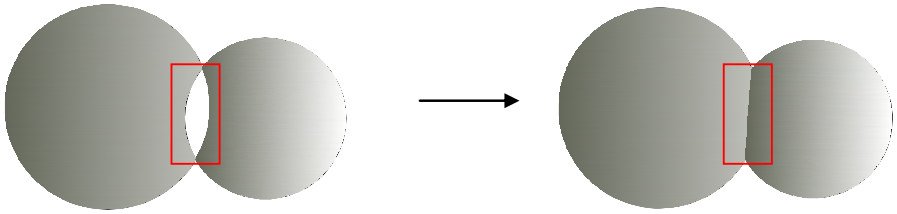

(a) (b)

This study can reveal the response of flowing wet foam to the plastic events in meso-level.